Aqueous dune-like bedforms in Athabasca Valles and neighbouring locations utilized in palaeoflood reconstruction

L. Durrant[1], M.R. Balme[1*], P.A Carling[2], P.M. Grindrod[3,4,5]

[1]School of Physical Sciences, Open University, Walton Hall, Milton Keynes, MK7 6AA, UK

*Corresponding author: matt.balme@open.ac.uk

[2]Geography & Environment, University of Southampton, Highfield, Southampton, SO17 1BJ, UK

[3]Department of Earth and Planetary Sciences, Birkbeck, University of London, London, UK

[4]Centre for Planetary Sciences at UCL/Birkbeck, London, UK

5Now at Department of Earth Sciences, Natural History Museum, London, SW7 5BD, UK

Abstract

Putative fluvial dunes have been identified within the Athabasca Valles and associated network of channels on Mars. Previous published work identified and measured bedforms in Athabasca Valles using photoclinometry methods on 2-3 m/pixel resolution Mars Orbiter Camera Narrow Angle images, and argued that these were created by an aqueous megaflood that occurred between 2 and 8 million years ago. This event is likely to have occurred due to geological activity associated with the Cerberus Fossae fracture system at the source of Athabasca Vallis. The present study has used higher resolution, 25 cm/pixel images from the Mars Reconnaissance Orbiter HiRISE camera, as well as stereo-derived digital terrain models and GIS software, to re-measure and evaluate these bedforms together with data from newly discovered neighbouring fields of bedforms. The analysis indicates that the bedforms are aqueous dunes, in that they occur in channel locations where dunes would be expected to be preserved and moreover they have geometries very similar to megaflood dunes on Earth. Dune geometries are used to estimate megaflood discharge rates, including uncertainty, which results support previous flood estimates that indicate that a flood with a discharge of ~2 x $10^6 m^3 s^{-1}$ created these bedforms.

Highlights

- Athabasca Valles bedforms have similar geometries to megaflood Earth aqueous dunes
- Earth-based dune height-length quantitative predictors fit well to Mars dunes
- Discharge estimates indicate a 2 million $m^3 s^{-1}$ megaflood deposited the dunes

Keywords

Megaflood; aqueous dune; flood estimate; Athabasca Valles; Mars

1. Introduction

Athabasca Valles is an outflow channel ~300 km long and ~20 km wide located in the Elysium Planitia region of Mars. The channel is thought to have been carved by a high-discharge flood of water, an interpretation based on features such as streamlined islands and a low number of tributaries (e.g., Burr et al., 2002a, 2002b), though some authors have suggested that fluid lavas might have carved it instead (e.g., Jaeger et al., 2010). Through examination of the topography and the consistent morphology of surface textures throughout the region, it is expected that flood waters originating from the Cerberus Fossae flowed along Athabasca Valles and debouched into the Western Elysium Basin (Balme et al., 2010), a flat floored basin of ~150,000 km2, and then 'filled and spilled' through smaller sub-basins, forming several other outflow networks, including the Lethe Valles system of channels and basins (Balme et al., 2011). Several authors (e.g., Jaeger et al., 2007; Keszthelyi et al., 2004; Plescia, 2003) have proposed that this flood-landscape was later infilled by fluid lavas, whereas others argue for a purely fluvial/lacustrine origin (i.e. debris covered ice, or textures related to the disappearance of a frozen lake) to form the present surface morphology (e.g., Brackenridge, 1993; Murray et al., 2005). Irrespective of whether the current surface is volcanic or ice-related, the majority consensus is that Athabasca Vallis was created by fluvial floods, although the hypothesis of it being carved by fluid lavas remains, and indeed this hypothesis has been proposed for outflow channels on Mars in general (Leverington, 2011).

The origin of the flood waters have been attributed to dike intrusions and faulting, leading to melting of large amounts of cryospheric ice (Berman and Hartmann, 2002; Burr et al., 2002a; Head et al., 2003; Plescia, 2003) which then carved Athabasca Valles. The 'pristine' appearance of the geomorphology, and measured impact crater size-frequency statistics suggest that flooding occurred as recently as 2–8 Ma (Burr et al., 2002b).

Putative subaqueous dunes (Burr et al., 2004) were identified using Mars Orbiter Camera Narrow Angle (MOC NA; e.g., Malin and Edgett, 2001) images in Athabasca Vallis. They occur in regions expected to have been inundated with flood waters, 60 km down-reach of the channel head (Burr et al., 2004). Burr et al., (2004) used photoclinometry to characterize dune morphometry and applied hydraulic modelling to these data to estimate the discharge of the palaeofloods. The MOC NA images used for this study had a spatial resolution of about 2 m per pixel, and the photoclinometry techniques they applied have some caveats (such as consistent albedo across the features being an assumption), however the authors concluded that the data were sufficiently good to support the hypothesis that the dunes were formed by the fluvial flooding, and that the discharge was ~2×10^6 m^3s^{-1}.

In this work, we test the hypothesis that these are flood-formed dunes as proposed by Burr et al., (2004) by applying a new dataset that provides better topographic information about the same dune field. Through the use of high resolution stereo images (from the High Resolution Imaging Science Experiment 'HiRISE'; , 25 cm/pixel; McEwen et al., 2007) from the Mars Reconnaissance Orbiter (MRO) spacecraft, we have been able to generate very high resolution (~1 m grid) digital elevation models of these dunes. We use these data to independently test the conclusions of Burr et al. (2004). Furthermore, we have found similar, apparently fluvial, bedforms in several other areas of this channel network (one more site in Athabasca Valles and two in Lethe Valles; Fig. 1) and have been able to create high resolution digital elevation models for two of these areas.

The first new site occurs in an overspill channel south of the main Athabasca Vallis and is about 200 km from source. The other two new sites are within Lethe Valles – the overspill system that allows return flow from the main Western Elysium Planitia basin to meet earlier overspills south of Athabasca (see mapping in Balme et al., 2010) and are over 600 km from the source region. We have called the areas studied by Burr et al., (2004) 'Site 1', the Athabasca overspill site 'Site 2', the upstream Lethe Vallis area 'site 3' and the

downstream Lethe Vallis area 'Site 4'. This study seeks to determine whether these newly found features are indicative of fluvial flooding in these areas. We use the morphometry data for the dunes to derive possible discharge values for the fluvial floods assumed to have formed these features, and compare with previous estimates of discharge.

2. Background

2.1 Young Martian Outflow Channels

Morphological features such as deeply incised channels, streamlined islands and cataracts and channel breaks have been identified that are strong indicators of the action of floodwaters on Mars (e.g., Baker, 1982; Baker and Milton, 1974; Burr et al. 2009). Many of these channel networks on Mars are ancient and were formed in the Noachian and Hesperian periods which are expected to have been able to support a more active hydrosphere (e.g., Carr, 2000; Craddock and Howard, 2002; Pollack et al., 1987). However, flood channels occur on Mars that seem to have been active in geologically recent times (the Amazonian epoch), including Mangala Valles (e.g., Basilevsky et al., 2009; Tanaka and Chapman, 1990) and Athabasca Valles (e.g., Berman and Hartmann, 2002; Burr et al., 2002b; Burr et al. 2009). Athabasca has been dated, based on impact crater statistics, as having formed within the last 10 million years (Burr et al., 2002b), although possible later infill by lavas (Jaeger et al., 2007; Plescia, 2003) and superposition relations with the Medusa Fossae Formation (Balme et al., 2010; Burr et al., 2002a), could suggest an older formation age.

The extension and fracture of the crust that formed the Cerberus Fossae (upper right of Fig. 1) might have released significant amounts of subsurface water, possibly as a result of dike emplacement (Head et al., 2003; Plescia, 2003; Vetterlein and Roberts, 2010). Examining the size and scale of Athabasca Valles and geomorphological features found within the channel allows inferences about the scale of flood waters to be

made, and about possible sequences of events. Recently Balme and Gallagher (2009) identified evidence for former ground ice in the head regions of Athabasca Vallis – suggesting that if episodes of volcanic and fluvial activity occurred, the fluvial flooding was probably the most recent, or that morphologies generated by ground ice were not completely erased by later volcanism.

2.2 Terrestrial megafloods as analogues for Mars

Landforms indicative of large scale, short-duration flood events occur in many locations on Earth (Carling et al., 2009a); including the Channelled Scablands in Washington State, USA (summarised by Baker, 2009), within the Altai mountains in Siberia (Carling, 1996a, 1996b), and deep underwater on the bottom of the English channel between France and the UK (Gupta et al., 2007; Gupta et al., 2017). These outflows contain features of a similar scale to those identified in Athabasca Valles, and are good analogues for catastrophic outflow channels on Mars in general. Hydraulic modelling, derived from palaeodischarge calculations of Earth flood events, have been used to estimate discharge rates on Mars (Leask et al., 2006; McIntyre et al., 2012; see also references in Wilson et al., 2009). Uncertainties in estimating floodwater heights in Martian outflow channels have created difficulties in estimating discharge, and hence the inferred discharge values range across orders of magnitude (see sensitivity analysis of McIntyre et al., 2012 for example). The results from various Martian studies have found discharge estimates that fall mainly between a range of 10^6 and 10^8 m^3s^{-1}, but which can be as high as 10^{10} m^3s^{-1} (Wilson et al., 2009) depending on assumptions made about water depths and flow regimes and the size of the system itself. Burr et al. (2004) used an approach based on the work of Carling (1996b), who noted that bedform size and shape can scale with flow velocity and depth, and so the use of bedform morphometry can give an estimate of flow depth independent of channel morphology, and hence a better discharge estimate.

Burr et al. (2004) used MOC image E10-01384 (3.1 m/pixel resolution) to argue that "channel-transverse dune-like bedforms, ten to a hundred meters in wavelength scale" were flood formed subaqueous

dunes rather than antidunes or aeolian dunes. They noted that "the blunt concordant outer terminations of the dunes, the dunes' contiguity to the streamlined form and their albedo appear more consistent with sub-aqueous formation (than aeolian)". Burr et al. (2004) used photoclinometry to measure the topography of these dunes and, by comparison of these data to Siberian flood-formed dunes (Carling, 1996b), argued that the Martian bedforms were comparable with the Siberian dunes in size and shape, and hence could be used to estimate flood discharge using the Carling (1996b) palaeohydraulic model. Using plausible estimates for grain size and bed roughness they calculated a discharge estimate of ~ 2×10^6 m^2s^{-1}.

3. Method

3.1. Creation of Digital Terrain Models from HiRISE stereo images

Of the four study areas, sites 1-3 had available HiRISE stereo images (the Athabasca Vallis area studied by Burr et al. (2004), the Athabasca overspill area, and the Lethe Vallis upstream region) at time of writing. The other area, the downstream Lethe Vallis area, has good coverage in CTX data but CTX-derived stereo products are of too coarse a resolution to be used in this study. We followed standard techniques to create the stereo DEMs (Kirk et al., 2008), using the Integrated Software for Imagers and Spectrometers (ISIS), freely-available through the United States Geological Survey (USGS), and the commercial software SOCET SET, available from BAE Systems. We produced stereo DEMs with a spatial resolution of 1 m/pixel and orthorectified images at 25 cm/pixel. We estimate the vertical precision of the DEMs using previous methods (Kirk et al., 2003; 2008; Okubo, 2010), the values of which are given in Table 1. In order to avoid analysis of interpolated data or DEM artefacts, we did not edit our DEMs after production, but instead highlighted and avoided any areas that contained artefacts. Such areas were identified using a hill-shade data product and the DEM itself. This approach was justified in this study, as there were very few artefacts (<<1% of DEM area) in the final DEMs, and none on or nearby any of the studied putative dunes.

147 *Table 1. HiRISE stereo observations and DEMs*

Site	Left Observation	Right Observation	Produced by	DEM Resolution (m/px)	Vertical Precision (m)
1	PSP_003294_1895	PSP_002661_1895	UoA	1	0.19
2	PSP_010045_1880	PSP_009768_1880	This study	1	0.10
3	PSP_006762_1840	PSP_010335_1840	This study	1	0.20
4	No HiRISE stereo coverage				

148

149 **3.2 Duneform morphometry**

150 The stereo derived DTMs were imported into ArcGIS software, together with the orthorectified images.
151 Putative dunes were identified visually, then topographic profiles created perpendicular to the crest of the
152 dunes to extract data along that line. These profiles provide data describing the dune shape (Fig. 3) and were
153 used to measure height (Hd), total length (L), stoss length (Ls) and lee length (Ls). Measurement error was
154 estimated to be +/- 1 image pixel. From these data, secondary data such as steepness (Hd/L), asymmetry
155 (Ls/Ll), and stoss and lee slope angles were calculated. When interrogating the DTM data with 25cm/pixel
156 orthoimages overlain, measurement error on horizontal distance was relatively small (+/- 25cm compared
157 with measurements of the order of 10m), but relative vertical error was greater, being similar to or slightly
158 less than the pixel size of the original images (Kirk et al., 2008) from which the DTM was created (table 1) for
159 measurements of the order of only a metre or so in height.

160 ***4. Observations and measurements***

161 **4.1. Observations of dune-like landforms**

162 Fig. 4 shows details of example dunes from each site as viewed in HiRISE images, revealing differences in
163 morphology. Some aspects of the dunes are common to all sites, however. For example, the crest ridges of
164 the putative dunes are generally transverse to the flow direction of any flooding, inferred from the shapes of
165 the channels and streamlined forms within them. The exception is site 3, discussed below, in which the dunes

have a rhomboid form. Also, the dunes occur near the margins of the channel, or close to islands or flow obstacles. There is a clear central channel region in each site in which the dunes either did not form, formed but were then swept away (and did not reform), or formed and were overlain by later flows or another infilling mechanism.

Site 1: The first area of putative aqueous dunes (Fig. 4a), described previously by Burr et al. (2004), is located approximately 60 km down slope from the Cerberus Fossae within the Athabasca Vallis main channel. This field of sinuous to linear ridges is ~ 6 km long and up to ~ 400 m wide. The proposed dunes are aligned transverse to the channel slope and are contiguous with a streamlined obstacle (apparently an eroded impact crater with a depositional tail) within the channel. The ridges have a wavelength of ~ 50 m and the morphology and scale of the bedforms are generally consistent along its length. The simple morphology of the dunes is disturbed in places by circular features sometimes described as Ring Mound Landforms (RMLs; Jaeger et al., 2007). The surfaces of the dunes are rough at metre-scale, giving them a "scaly" appearance. The areas between the dunes have a similar texture, except for some smooth, bright regions. Ninety topographic profile measurements of these bedforms were made across the dunefield. Typically, the dunes are ~ 50 m in length and ~3 m height. Stoss slope lengths average ~ 33 m and are typically greater than lee slope lengths (average ~ 17 m) giving a mean asymmetry of 1.9. The largest bedform is ~ 94 m long and the tallest 5.5 m high.

In addition to the ridge-like "2D" dune forms at site 1, a small number (9) of more isolated "3D" dune forms were analysed. These have mean length of ~ 63 m and mean height of ~ 4 m, and a mean asymmetry of 1.3. All these data are summarised in table 2.

Site 2: The second site, where we made a new identification of possible dunes, is located within a network of channels that are shaped by an overspill from the main Athabasca Valles channel. This overspill is ~ 200 km from the Cerberus Fossae origination point along the main Athabasca Valles channel. The dunes are ~ 16 km south of the overspill point and are located at a point where two or more sub-channels in this network meet. There appear to be several groups of flood dunes in this area in the lee of obstacles (Fig. 2b), which is similar in setting to pendant bars seen behind obstacles in terrestrial flood environments (Baker, 2009), although the dune morphologies are more transverse than flow parallel in this case. In the clearest examples, the morphology is similar to the dunes measured in area 1 (i.e. channel-transverse, sinuous to linear ridges); the morphometry of this group has been measured in detail. There are about ten transverse bedforms in this series, with those at the downstream end being more well-defined, but smaller. The dunes decrease in length along the direction of flow (from ~ 80 m to ~34 m) but do not change in mean height (2.2 m compared to 2.3 m). However, the interdunal space increases as the length of the dunes decrease. This may be due to infilling from subsequent flows or later, possibly aeolian, material which, on Earth, can fill dune troughs (Carling, 1996a; Carling et al., 2016) increasing dune spacing and decreasing the apparent height of dunes. This pattern is somewhat different to site 1, where there was little change in dune length with distance down flow. The morphometry data are summarised in table 2. HiRISE images (Fig. 4b) reveal that the dunes do not have a rough texture like those in site 1, but do have a subtle pattern of polygonal troughs on their stoss sides. This texture is also found on the interdune areas and on the surrounding channel floors.

Site 3: The third area where possible flood-formed dunes have been identified is in Lethe Valles, ~ 120 km from the overspill point from the Western Elysium basin, and just downstream from a cataract system(see Balme et al., 2011, 2010). This field of features is ~ 3 km long and ~ 400 m wide. It occurs in, and downstream of, a smaller side channel to the main flow; the putative dunes are enclosed on one side by the channel edge (Fig. 2c). These forms have a distinctive morphology that differs from the other dunes identified in this study as they do not have a traditional dune crest-ridge shape in plan-view. They do, however, clearly possess

shallow upstream sides, and steep downstream faces, and so resemble 'rhomboid' (sometimes called 'chevron') dunes that occur in transcritical flows (Allen, 1982, Vol. 1). The maximum height for this series of features is 7.2 m, which is almost as high as the depth of the channel here (approximately ~10 m deep to one possible morphological channel margin, or ~ 17 m depth to an alternative channel margin). The bedforms have very low steepness (0.2), are very asymmetrical (2.95), and therefore have very shallow stoss slopes with a mean of 1.7° and maximum of 2.6°. When viewed in HiRISE images (Fig 4c), the features are smooth and have subtle polygonal- patterned upper surfaces, similar to those of the dunes in site 2. This texture is also found on the eastern channel margin (the channel floor is infilled by later, rougher, blocky material). The surfaces of the rhomboids also contain narrow (< 1 m) lineaments or subtle troughs that are very straight, which can sometimes extend for great distances (up to hundreds of metres), and which sometimes cut across several 'bedforms'.

Site 4: This site is located ~ 30 km further along the Lethe Vallis channel from site 3 and appears to host more fields of dune like forms (Fig. 2d). These bedforms occur on either side of the channel, at a point where it widens after going around a streamlined island that is ~ 7 km long and ~ 1.5 km wide. The dune-like forms are larger than at sites 1 and 2, with distances between crests of several hundred metres. The bedforms are crescentic in plan-view shape, and have a steep downstream side and a shallower stoss side. The crest-ridges tend to be oblique to the channel thalweg, with the normal to the crest pointing slightly into the centre of the channel. At the time of writing there was no HiRISE DEM available for this area. Overall, the features here appear to be subdued, with shallower slopes than the other sites, but without high-resolution DEM data, this topography can only be assessed qualitatively. These features have the same surface texture (Fig. 4d) as the rhomboid features in site 3: smooth surfaces with subtle polygonal textures and faint lineations.

4.2 Morphometry of possible dune features

233 For the three sites with HiRISE DEM coverage, we measured the shape of the putative dunes. For site 1,
234 we measured the same set of features as studied by Burr, et al. (2004), but used a completely different type
235 of topography data (derived from stereo photogrammetry, rather than shape from shading). This allows us
236 to test Burr et al.'s data, and provide a robust test of their dune hypothesis. We also compared the proposed
237 bedforms in Athabasca to previous data for terrestrial dunes used in work on the palaeohydrology of the
238 Kuray (Siberia) flood-formed dunes (Carling, 1996a, b). Table 2 shows a summary of the data collected in this
239 study, together with the data of Burr et al. (2004) and the Carling (1996b) Siberian dunes data. The measure-
240 ment data were obtained from profiles as described above and shown in Fig. 3.

241

242 *Table 2. Comparison morphometric data for this study and previous studies on Earth and Mars. * = weighted*
243 *means used as measurement errors were not the same for each datum.*

	Past studies		This study			
	Kuray Dunes (Carling, 1996b)	Athabasca Site 1 (Burr et al., 2004)	Site 1 Athabasca main channel 2D dunes	Site 1 Athabasca main channel 3D dunes	Site 2 Athabasca overspill	Site 3 Lethe Valles rhomboids
Data points	N/A	75	91	9	26	11
Max height (m)	~16	~5.1	5.5	5.6	3.5	7.2
Mean height, H_d (m)	N/A	N/A	2.9	4.1	2.0	3.8
Max length (m)	~200	~130	94	86	83	380
Mean length, L (m)	N/A	N/A	50	63	40	200
# with longer stoss than lee	~85%	~90%	~86%	~ 66%	~85%	~91%
Mean steepness*	0.029	0.055	0.057	0.065	0.051	0.020
Max steepness	~0.12	~0.12	0.090	0.091	0.11	0.032
steepness st. dev.	0.016	0.016	0.017	0.013	0.02	0.006
Mean asymmetry*	N/A	N/A	1.20	1.3	1.3	3.0
Max asymmetry	N/A	N/A	7.4	2.9	9	6.6
Asymmetry st. dev.	N/A	N/A	1.4	0.66	1.5	1.67
Stoss angle range	3-10°	4-14°	2-11°	5-9°	2-14°	1-3°
Mean stoss angle*	N/A	N/A	4.8°	6.7°	4.0°	1.6°
Lee angle range	>3°, 17-19°	8-20°	4-23°, 1 outlier of 37°	6-16°	4-15°, 1 outlier of 40°	3-8°
Mean Lee angle*	N/A	N/A	8.8°	9.2°	6.4°	1.9°

244

The site 1 and 2 dune candidates are similar in size and form, being generally a few metres high and a few tens of metres long (Fig. 5, 6). Their stoss slopes are about half as steep as their lee slopes and are generally a few times longer in planview. There is little difference between site 1 and 2 – site 2 has slightly smaller and lower features, but they generally plot in the same area on an asymmetry/steepness plot (Fig. 5). The asymmetry/steepness data for sites 1 and 2 are very close to those values shown in Figure 10 of Carling et al. (1996b) showing a similarity in form between the two data sets. This consilience was also found by Burr et al. (Burr et al., 2004; fig 6). The site 3 features are different though, as shown both by their morphology described above, and in their size and form. They are generally longer (a few hundred metres in length) and about twice as high but flatter (Fig. 6). It is clear from both morphology and morphometry that the site 3 features are distinct from the site 2 and 3 features. We have no morphometry data for site 4, but do note that they are larger than the site 1 or 2 features.

5. Analysis

5.1 Morphology and morphometry

Burr et al. (2004) detail the arguments for the site 1 dune-like features being aqueous dunes and a brief additional discussion is provided here. Visually the landforms studied in this paper appear similar to examples of terrestrial analogues, such as the Kuray dunes and the dunes in the Washington scablands (e.g., Baker, 2009; Carling, 1996b). The site 1 and site 2 features in the Athabasca main channel and overflow areas are particularly similar in morphology to terrestrial flood-formed dunes. The data in Table 2 also shows the morphometry is comparable in shape and size to terrestrial flood-formed dunes (table 2 and Fig. 5). The positioning of these dunes within a channel contiguous to a feature that is indicative of flow (a streamlined island in site 1 and an overspill channel in site 2) add support to this interpretation. In Site 1, the direction at which

267 the dune field extends is from roughly NE to SW. The prevailing winds in this region are SE to NW (Burr et al.,
268 2004) which argues against these being aeolian dunes.

269 The possible bedforms identified in site 3, the Lethe Valles channel (Figs. 2c and 4c), share similarities
270 to the Athabasca Valles dunes discussed above but have an exaggerated asymmetry (Fig. 5) and the appear-
271 ance of rhomboid dunes, which are created in a different flow regime. It has been suggested that this type
272 of dune forms in transcritical flows with a Froude number ~ 1, in narrow channels, and where hydraulic jumps
273 may be present (Chang and Simons, 1970). This environment matches the characteristics in the Lethe Valles
274 channel where these bedforms appear.

275 Our data are similar to those obtained by Burr et al. (2004) obtained using a different topographic
276 dataset and lower resolution imaging data. We find that both site 1 and site 2 dunes occupy similar morpho-
277 metric parameter spaces and, as found by, nearly all of the putative dunes from sites 1 and 2 plot to the right
278 of a power function with an exponent of 0.84 in a height/length plot. The site 3 features are even flatter,
279 and plot far to the right of this line.

280 **5.2 Estimates of palaeoflow characteristics**

281 The application of hydraulic modelling to Martian channel systems can be limited by a lack of knowledge
282 of flow depth. Where channel bedforms (such as dunes) exist, flow depth may be estimated independently
283 of channel morphology. Carling's (1996b) hydraulic modelling method used dune morphology to estimate
284 flow depth, and was used by Burr et al. (2004) for Mars. This model requires data describing bed roughness
285 (Manning's friction coefficient) and grain size but this information is generally unavailable for the Martian
286 surface, and estimates must be used instead. Although HiRISE image resolution is sufficient to give an im-
287 pression of the largest channel floor particles, there is no way of knowing if this is representative of the
288 surface during flow, or if channel beds have been infilled by late-flood sediments, later lavas, or have gained
289 a thick covering of dust or sand since the flood event. This observation makes it difficult, perhaps impossible,

290 to know the bed roughness or the average grain size at present. Burr et al. (2004) estimated these factors for
291 their discharge calculations, as have other researchers (e.g., Kleinhans, 2005; McIntyre et al., 2012; Wilson
292 et al., 2009), using whatever information is best available.

293 Noting these difficulties, we have used a simple set of conditions and equations based on dune mor-
294 phology alone to make a first order estimate of discharge. We first assume that these bedforms are dunes,
295 rather than antidunes. This assumption seems a reasonable, given the measured asymmetries, as dunes
296 should have longer stoss than lee slopes (see also arguments presented for site 1 by Burr et al., 2004). We
297 calculate discharge by (i) first estimating flow depth, from measurements of dune length, (ii) estimating flow
298 speed from Froude numbers inferred from dune morphology, and then (iii) combining these data with meas-
299 ured channel widths to give discharge.

300 Flow depths have been estimated from dune length measurements. Many authorities have noted
301 that flow depth scales with dune height and length. We follow Julien and Klaassen (1995) and van Rijn (1984),
302 who find that, for simple dunes with a consistent cross section across a channel section ("2D dunes"), the
303 following approximation applies:

304 $$L = \alpha 2\pi h \quad (1)$$

305 where L is dune length, □ a constant, and h is flow depth. Carling (1996b) notes that significant variation
306 exists in this relationship represented in the equations by a range of values for α, where α is 0.7 for develop-
307 ing gravel-dunes, falling to 0.4 for the steepest dunes. Values for α of 0.6 to 1.1 are given for fluvial sand
308 dunes. We assume that α = 0.7 because, at least for site 1 and site 2, the dune steepness values are ~0.05 to
309 0.06, consistent with the steepness of 'developing' gravel-dunes given in Carling (1996b).

310 Next, because dunes form when flow is sub-critical (as opposed to antidunes, the bedforms gener-
311 ated when flow is critical to supercritical) we assume the Froude number of flow was between ~ 0.45 to ~

312 0.84, based on the review of the formation of coarse-grained (gravel) aqueous bedforms of Carling (1999)
313 and in accord with the flow modelling of Athabasca Vallis by Burr (2003) where calculated Froude number
314 was typically 0.5. We can then use the expression for Froude number to calculate approximate flow speeds.
315 Froude number (Fr) is given by

316 $$F_r = \frac{v}{\sqrt{gh}} \quad (2)$$

317 where v is flow velocity, g is gravity. Combining (1) and (2) gives

318 $$v = F_r \sqrt{\frac{gL}{\alpha 2\pi}} \quad (3)$$

319 and hence discharge can be calculated as

320 $$Q = vhw \quad (4)$$

321 where w is the width of the flow.

322 These simplified discharge estimate equations were tested against the more complete model of Car-
323 ling (1996b), who estimate the paleodischarge data of floods that formed dunes in the Kuray dunefield in the
324 Altai Mountains Siberia. Carling (1996b) gives a peak discharge estimate of 7.5×10^5 m^3s^{-1} for the floods that
325 formed the dunes. The maximum dune length in this field is 200m with a height of 16m, and a 'field width'
326 of 2400m (Carling, 1996b). Using these data with the simplified equation (3) and assuming a Froude number
327 between 0.45 and 0.84, gives a discharge of between 6.4×10^5 m^3s^{-1} and 1.2×10^6 m^3s^{-1}, comparing well with
328 Carling's discharge value. Indeed, Carling (1996b) states "It should be emphasized that the model indicates
329 the probable scale of palaeoflows and not absolute values. Nevertheless, even allowing for parameter un-
330 certainty, it appears that the discharge over the Kuray dunefield was probably about 7.5×10^5 m^3s^{-1} and need
331 not have exceeded 10^6 m^3s^{-1} with a water depth of only a few tens of metres." In this case, it would seem

reasonable that the simplified equations for discharge would be adequate given the limitations of the Mars data available and the purposes of this study.

Site 1. Main Athabasca Channel

The mean dune length in site 1 is 50 m (table 2). Assuming Froude numbers of 0.45 - 0.84, the values obtained for v are ~ 3.0 to 5.5 ms^{-1}, with a flow depth of about 11 m. Importantly, the dune heights as measured are below this depth. The longest dune length measured in site 1 was 94m, about double the mean. Using this largest value for length in (3) gives values for v of 4.0 to 7.5 ms^{-1}, with flow depths of ~ 21 m. Again, the measured height of this dune is less than the estimated flow depth. Given that the channel here is about 19 km wide, discharge, Q, can be estimated as being between 6.4×10^5 m^3s^{-1} to 1.2×10^6 m^3s^{-1} for the mean dune length, or 1.6×10^6 m^3s^{-1} to 3.0×10^6 m^3s^{-1} for the longest dunes. These latter data are close to the discharge estimates of Burr, et al. (2004), who found peak values of ~ 2×10^6 m^3s^{-1} using a fuller hydraulic model based on Carling (1996a,b). The similarity of the values is consistent with the hypothesis that the dunes are consistent in length and height being formed due to a flood of this magnitude of discharge.

Site 2. Athabasca overspill area

There appear to be up to nine transverse ridges at this site, making a pattern of dunes similar to the "2D dunes" in site 1. The ridges become progressively shorter in length and less wide along the direction in flow (see Fig. 4b). The ridges also become discontinuous. This morphological adjustment probably is due to the confluence of another branch of the overspill channel. Although the dunes get progressively shorter and narrower along the dune field they do not appear to reduce in height. They get steeper, and more fragmented in morphology, so they become more like isolated "3D" dunes than ridge-like bars. 3D dunes tend to form at lower Froude numbers (Carling, 1996a), representing less turbulent and relatively deeper (compared to their

velocity) flows. We apply the same technique to estimate discharge as we did for site 1, but note that this may not be applicable for these dunes further down-stream.

For the dune ridges furthest upstream in site 2, the largest dune length is 83m with a dune height of 3.5 m. Applying Equations 1-3 with Froude numbers of 0.45 to 0.84, to these values gives a flow speed 3.8 to 7.1 ms^{-1} and flow depth of about ~19 m. Using the mean values for length of 40 m, the calculated flow speeds are 2.6 to 4.9 ms^{-1}, with a flow depth of ~ 9 m. If the 3D shape of the dunes at the downstream end of this channel reach are representative of lower Froude number flow then this, together with their shorter lengths, suggests much slower flow speeds here than 500m or so up stream. This reduction in flow rate is probably because of the convergence of several narrower channels to one larger, broader channel here (Fig. 7). Using the mean dune length, the lower, more conservative, Froude number for flow speed here, and the calculated depth and measured 7 km width of the channel (just downstream of C in Fig. 7) gives a discharge of about 1.7×10^5 m^3s^{-1}. Using data for the smallest dunes in the downstream part of the flow, discharge is only ~4.7×10^4 m^3s^{-1}. In contrast, using the Froude numbers of 0.45 to 0.84 again, perhaps more applicable to the upstream dunes, gives discharge values of 5×10^5 m^3s^{-1} to 9×10^5 m^3s^{-1}.

Site 3 – Lethe Valles Rhomboid dunes

Rhomboid dunes usually form in shallow fast moving flows where the Froude number ~ 1, so flow is transcritical above both sand beds (Chang and Simons, 1970; Allen, 1982, Vol. 1, p. 405) and gravel beds (Ikeda, 1983), such as where there is sudden channel widening or deepening, or in a narrow channel where oblique standing waves may occur. In experimental flows above sand beds, rhomboid dunes were also associated with superimposed linear grooves (Karcz & Kersey, 1980) as noted at this location. In the case of the

Lethe Valles, the putative rhomboid dunes are found at a location where conditions might have existed which match the terrestrial setting of rhomboid dunes. The dunes form at the point at which two channel-segments, separated by a streamlined island, reconverge. They form immediately against the side of the channel. Also, where the dunes begin, there are a series of topographic obstacles and roughness elements (probably bed-rock remnants) which might have caused a hydraulic jump in the flow. This topographic setting may have been enough to have set up an oblique standing wave, allowing such dunes to form. The channel where these dunes occur is ~ 2km to 2.5 km wide and at most ~17 m deep (Balme et al., 2011) but, depending on where one interprets the flow surface to be, based on the topographic profile, the 'active' depth could have been as little as 10 m; see Fig. 8. If these are rhomboid dunes, then their morphology indicates relatively shallow flows (Chang and Simons 1970; Karcz and Kersey 1980) of water above the top of the dunes.

The turbulent nature of the flow suspected to create these type of dunes makes the equations used for site 1 and 2 inappropriate for this area. A very approximate estimate of discharge can be made, though: if these forms were generated in a flow with Froude number of ~1.0 and an approximate channel depth of 10-17 m, then, from (2), the flow velocity was about 6-8 ms^{-1}. With a channel width of ~2 km, discharges of 1.2×10^5 - 3×10^5 m^3s^{-1} would have occurred. These values are more than twice the discharge estimate for Lethe Vallis as a whole (1×10^4 - 5×10^4 m^3s^{-1}) made by Balme et al. (2011). The discrepancy could be because these dunes formed during peak discharge with high Froude numbers, whereas the whole-channel estimate is based only on the slope, depth and estimated roughness of the channel.

6. Discussion

6.1. Comparison with previous Martian studies

The morphometry data shown in table 2 and Figs. 5 and 6 demonstrate a close similarity between the results gathered from a HiRISE DEM (this study) and from MOCNA photoclinometry (Burr et al., 2004). This

reanalysis validates the arguments and analysis of Burr et al. (2004) and their conclusion that these are flood-formed dunes and is consistent with the flow modelling conducted by Burr (2003). Our data from the nearby site 2 plot in the same positions as the site 1 data in two different parameter spaces (asymmetry-steepness, and length-height). Also, the dune-like forms here have a similar morphology and setting to those in site 1. We conclude that these landforms formed in the same way as those in site 1. This outcome adds further credence to the conclusion that Athabasca Vallis and its tributary channels were formed by (or at least were the conduits for) aqueous floods, and that sub-aqueous dunes formed during such flows.

Calculations using data gathered from site 1 give an estimated dune forming discharge of about 6×10^5 to 3×10^6 m^3s^{-1}. This discharge range is close to the estimate of Burr et al. (2004) who estimate that discharge was 7.5×10^4 m^3s^{-1} at the start of dune formation, increasing to 2.1×10^6 m^3s^{-1} at the peak of the flood. Burr et al. (2004) used both a different dataset and a fuller hydraulic modelling approach, but our simple dune morphometry-based calculations provides reassurance both that these features are consistent with formation in a megaflood, and that the peak flood discharge in Athabasca was around 10^6 m^3s^{-1}. Again, our analysis supports the conclusions of Burr et al. (2004), despite using a different model and a different dataset.

Interestingly, the inferred discharge in site 2 (4.7×10^4 to 9.4×10^5 m^3s^{-1}), a smaller, distributary overspill channel, is only about an order of magnitude less than that of the main channel discharge. This result probably reflects the fact that this zone is a convergence of several smaller overspill channels: McIntyre et al. (2012) found discharge values of ~ 4×10^4 to 1.4×10^5 m^3s^{-1} for a single overspill channel conduit near the source region of Athabasca Vallis. The relatively high site 2 discharge could indicate peak flow conditions, or a relatively brief period of overspill before the main Athabasca channel was down-cut enough to abandon this channel. Either way, these data suggest that even the overspill channels associated with Athabasca Vallis hosted significant flows with discharges of ~ 10^5 m^3s^{-1}.

6.2 Comparison with terrestrial studies

Carling (1999) collated a large data set of dune height (H) and lengths (L) for gravel dunes formed in experimental channels, in rivers and in palaeofloods. Notably these dunes all developed in water. An appreciation of the data trends demonstrated that the growth of 2D dunes tended to follow the trend:

$$H = 0.0073L^{1.5} \quad (5)$$

which is plotted in Fig. 6. When developing for long enough in sustained flows, dunes tend to develop maximum steepness; i.e. maximum heights for minimum length. The upper limit to steepness has been described by Ashley et al. (1990) as $H = 0.16\ L^{0.84}$ for dunes formed in sandy beds and as:

$$H = 0.18L^{0.84} \quad (6)$$

for gravel dunes (Carling, 1999); which trend is plotted in Fig. 6.

The Site 1 dunes tend to be 2D forms, transverse to the flow and, despite scatter, are evenly spread across the trend of Equation 5. Some are of shorter span; Site 1 dunes exhibit more 3D forms and tend to plot above Equation 5. Site 2 dunes are also transverse but again those that exhibit a more 3D form also plot above Equation 5. The Lethe rhomboid dunes at site 3 are evidently low-amplitude non-equilibrium forms developed in unsteady flows as described above.

It is evident that the Martian 2D bedforms not only generally develop steepness in accord with Equation 5, which pertains to gravel dunes on Earth, but steeper dunes, which tend to be 3D, also conform to the steepness limit appropriate for water-lain gravel dunes (Equation 6). The accordance of the behaviour of Martian and Earth bedforms could be fortuitous, but the conformity is remarkable and is a strong indicator that the Martian bedforms are alluvial dunes and probably are formed in gravel rather than sand. Such a conclusion is a strong argument for the former presence of large water floods on the Martian surface. In addition, the consilience in the behaviour of flow and the deformation of the channel bed to form dunes on both Mars

441 and Earth is consistent with the classical arguments of Komar (1979; 1980). Komar (1979; 1980), Burr et al.
442 (2006) and Carling et al. (2009a) have argued that the application of fluid mechanics equations developed for
443 terrestrial environments is appropriate for Martian environments as both systems are subject to the laws of
444 physics.

445 **6.3 New areas containing dunes**

446 The identification of new areas (sites 2 to 4) containing landforms of similar morphology to those in site
447 1 add further weight to the interpretation that there were dune-forming floods in this system. The similar
448 morphology, morphometry and inferred discharge values from sites 1 and 2 all support this conclusion. As
449 described by Burr et al. (2004), other explanations (such as aeolian deposition) do not explain the morphology
450 or setting of the dunes. This is especially true in our site 2, where dunes are observed associated with stream-
451 lined remnants in the flow. The interpretations for sites 3 and 4 are more equivocal: the rhomboid dunes
452 hypothesis for site 3 is compelling in that these features appear to be found in a setting appropriate to the
453 interpretation. However, it must remain only a working hypothesis until further good terrestrial (or perhaps
454 Martian) analogues can be found, for it is difficult to judge whether their morphology is consistent with aque-
455 ous floods on Earth, or if there is another explanation (perhaps as erosional forms within the flood; Carling
456 et al., 2009b) for these distinctive morphologies. The interpretation for Site 4 is also inconclusive due to the
457 lack of good terrain data. Here, though, the downstream pattern of the features, and their restriction to
458 within the channel, argues strongly that they were formed in association with flow of a fluid through Lethe
459 Vallis. Again, though, without topographic information at the required scale it is uncertain whether these are
460 depositional sedimentary features, as it is possible that they could be some kind of flood-formed erosional
461 feature, such as pseudo-dunes (Richardson & Carling, 2005) eroded into the bedrock. We must restrict our-
462 selves to concluding that at least some of the forms here are consistent in planview morphology and scale to
463 flood-formed sedimentary dunes. Not least the asymmetry (Fig. 4d) and the strong skewing of the crestlines

464 (Figs. 2d and 4d) of the site 4 bedforms with respect to the assumed flow direction is consistent with aqueous
465 dunes forming in a strongly three-dimensional flow field (Allen, 1984, Vol. 2 p. 145; Rubin and Ikeda, 1990).
466 A strongly developed three-dimensional flow is consistent with the location of the bedforms on the outside
467 of a channel bend. Taken together, though, the evidence appears to be more compelling: within this very
468 large system of erosional channels there are several, widely separated, examples of features that can be
469 interpreted as flood-formed dunes, and that, for at least one site, this interpretation is robust when analysed
470 using two different datasets.

471 **6.4 Significance of identification of flood-formed dunes.**

472 These results lend further support to the conclusion that one or more megaflood events flowed down
473 the Athabasca Valles due to geological activity at the Cerberus Fossae. This, in turn, adds further evidence
474 for, in the recent past, there having been significant subsurface water in local aquifers (Burr et al., 2002a;
475 Hanna and Phillips, 2006; Head et al., 2003; Manga, 2004) that provided water for the floods. Although it has
476 been proposed that these dunes were later coated in a thin veneer of lava (e.g., Jaeger et al., 2007), dunes
477 are not features that can be formed by flowing lava. Hence, it is likely that these features are sedimentary in
478 the main part. This is itself of interest from an astrobiological point of view. Although the cold, dry high UV
479 radiation surface (Horneck, 2000; Smith and McKay, 2005) conditions on Mars today arguably make it unlikely
480 to support life of any kind now or in the recent past, a subsurface aquifer provides a much more promising
481 habitat (Fisk and Giovanni, 1999), especially in a setting where there is evidence of volcanic activity that could
482 have provided heat and energy, perhaps as a hydrothermal system. Sediments deposited in flood-formed
483 features such as dunes might themselves have originated from within such habitats, and any water-ice pre-
484 served deep within the dunes (especially if later covered and protected by a thin crust of lava) would certainly
485 have come from this aquifer. Some of the lithic materials that compose the dunes could also have been
486 sourced from deep underground from within possibly habitable environments. Hence, drilling into these

flood-formed dunes would provide an opportunity to search for biomarkers from a recent subsurface, possibly habitable environment which could have supported a biosphere (Fisk and Giovannoni, 1999).

7. Conclusions

(1) The current analysis, using improved resolution DEMs (from HiRISE stereo imagery vs MOC photoclinometry), supports the conclusion of Burr et al. (2004) that there are aqueous flood-formed dunes in the main Athabasca Valles channel.

(2) Previously undescribed sets of landforms found in other channels associated with Athabasca Vallis are also likely to be flood-formed dunes.

(3) In Lethe Vallis, an overspill channel from a large basin further downstream from Athabasca, bedforms have a distinctive rhomboid morphology that is consistent with some examples of terrestrial aqueous dunes that form in high Froude number transcritical flows.

(4) Morphometric data were used to estimate discharge in the dune-forming floods. We used a, simple first-order method to estimate discharge that differs from that employed by Burr et al. (2004) but the results are similar. This outcome gives credence to the hypothesis that the features in this location are indeed subaqueous dunes and formed in a large flood event.

(5) Notably, bedform steepness on Mars develops in accord with the growth of gravel dunes on Earth; reaching a limit to maximum steepness limit that is remarkably consistent with that observed for water-lain dunes on Earth.

(6) Taken together, these observations and calculations strongly support the hypothesis of a large scale flood or floods originating from the Cerberus Fossae, flowing down Athabasca Valles into the Western Elysium basin, then filling and spilling into Lethe Valles and other channels.

(7) Finally, if the floods that formed these dunes had their origin in a subsurface aquifer, then they might, even now, contain materials (ice and sediment) from within this aquifer. As such sub-surface Martian environments are possibly habitable these flood-formed dunes might be good targets for future astrobiological exploration as they could preserve biosignatures from a subsurface biosphere, if such exists.

8. Acknowledgements

MRB was supported by the UK Space Agency (grants ST/F012020/1 and ST/L00643X/1). PMG was supported by the UK Space Agency (grants ST/L00254X/1 and ST/J005215/1). The stereo DEM processing was carried out at the UK NASA Regional Planetary Image Facility (RPIF) at University College London. We thank an anonymous reviewer for suggestions that improved the manuscript.

517 ***9. References***

518 1 Allen, J.R.L., 1982. Sedimentary Structures: their Character and Physical Basis, Vols. 1 and 2. Elsevier, Am-
519 sterdam.

520 2 Ashley, G.M., 1990. Classification of large-scale subaqueous bedforms: a new look at an old problem. Jour-
521 nal of Sedimentary Petrology 60, 160–172.

522 3 Baker, V.R., Milton, D.J., 1974. Erosion by catastrophic floods on Mars and Earth. Icarus 23, 27–41.

523 4 Baker, V.R., 1982. The Channels of Mars. University of Texas Press, Austin, Texas.

524 5 Baker, V.R., 2009. Channeled Scabland morphology, in: Burr, D.M., Carling, P.A., Baker, V.R. (Eds.), Mega-
525 flooding on Earth and Mars. Cambridge University Press, Cambridge, pp. 65–77.

526 6 Balme, M.R., Gallagher, C., 2009. An equatorial periglacial landscape on Mars. Earth Planet Sci Let 285, 1–
527 15.

528 7 Balme, M.R., Gallagher, C., Page, D.P., Murray, J.B., Muller, J.-P., Kim, J.-R., 2010. The Western Elysium
529 Planitia Palaeolake, in: Cabrol, N. (Ed.), Lakes on Mars. Elsevier, New York, pp. 275–305.

530 8 Balme, M.R., Gallagher, C.J., Gupta, S., Murray, J.B., 2011. Fill and spill in Lethe Vallis: a recent flood-routing
531 system in Elysium Planitia, Mars. Geol. Soc. Lond. Spec. Publ. 356, 203–227. doi:10.1144/SP356.11

532 9 Basilevsky, A.T., Neukum, G., Werner, S.C., Dumke, A., van Gasselt, S., Kneissl, T., Zuschneid, W., Rommel,
533 D., Wendt, L., Chapman, M., Head, J.W., Greeley, R., 2009. Episodes of floods in Mangala Valles, Mars,
534 from the analysis of HRSC, MOC and THEMIS images. Planet. Space Sci. 57, 917–943.
535 doi:10.1016/j.pss.2008.07.023

536 10 Berman, D.C., Hartmann, W.K., 2002. Recent fluvial, volcanic and tectonic activity on the Cerberus Plains
537 of Mars. Icarus 159, 1–17.

538 11 Brackenridge, G.R., 1993. Modern shelf ice, equatorial Aeolis quadrangle, Mars. Lunar Plan Sci Conf XXIV,
539 Abstr. # 175.

540 12 Burr, D.M., Grier, J.A., McEwen, A.S., Keszthelyi, L.P., 2002a. Repeated aqueous flooding from the Cer-
541 berus Fossae: evidence for very recently extant, deep groundwater on Mars. Icarus 159, 53–73.

542 13 Burr, D.M., McEwen, A.S., Sakimoto, S.E.H., 2002b. Recent aqueous floods from the Cerberus Fossae,
543 Mars. Geophys Res Lett 29, doi:10.1029/2001GL013345.

544 14 Burr, D.M., 2003. Hydraulic modeling of Athabasca Vallis, Mars. Hydrological Sciences Journal 48, 655–
545 664.

546 15 Burr, D.M., Carling, P.A., Beyer, R.A., Lancaster, N., 2004. Flood formed dunes in Athabasca Vallis, Mars:
547 morphology, modeling and implications. Icarus 171, 68-83.

548 16 Burr, D.M., Emery, J.P., Lorenz, R.D., Collins, G.C., Carling, P.A., 2006. Sediment transport by liquid over-
549 land flow: application to Titan. Icarus 181, 235-242.
550 17 Burr, D.M., Wilson, L., Bargery, A. S., 2009. Floods from Fossae: a review of Amazonian aged extensional-
551 tectonic megaflood channels on Mars In: Burr, P.A. Carling and V. Baker (Editors), Megaflooding on Earth
552 and Mars. Cambridge University Press. Cambridge, UK, pp 194-208.
553 18 Carling, P.A., 1996a. Morphology, sedimentology and palaeohydraulic significance of large gravel dunes,
554 Altai Mountains, Siberia. Sedimentology 43, 647–664.
555 19 Carling, P.A., 1996b. A preliminary palaeohydraulic model applied to Late-Glacial gravel dunes: Altai
556 Mountains, Siberia, in: Branson, J., Brown, A.G., Gregory, K.J. (Eds.), Global Continental Changes: The
557 Context of Palaeohydrology, Geological Society Special Publications. London, UK, pp. 165–179.
558 20 Carling, P.A., 1999. Subaqueous gravel dunes. J. Sediment. Res. 69, 534–545. doi:10.2110/jsr.69.534
559 21 Carling, P.A., Johnson, T. and Brennan, T. 2009a. A review of open-channel megaflood depositional land-
560 forms on Earth and Mars In: Burr, P.A. Carling and V. Baker (Editors), Megaflooding on Earth and Mars.
561 Cambridge University Press. Cambridge UK, pp 33-49.
562 22 Carling, P.A., Herget, J., Lanz, J.K., Richardson, K. and Pacifici, A. 2009b. Channel-scale erosional bedforms
563 in loose granular material and in bedrock In: Burr, P.A. Carling and V. Baker (Editors), Megaflooding on
564 Earth and Mars. Cambridge University Press. Cambridge UK, pp 13-32.
565 23 Carling, P.A., Bristow, C.S., Litvinov, A.S. 2016. Ground-penetrating radar stratigraphy and dynamics of
566 megaflood gravel dunes. Journal of the Geological Society 173, 550-559.
567 24 Carr, M.H., 2000. Martian oceans, valleys and climate. Astron Geophys 41, 3.20–3.26, doi: 10.1046/j.1468–
568 4004.2000.00320.x.
569 25 Chang, H.Y., Simons, D.B., 1970. The bed configuration of straight sand-bed channels when flow is nearly
570 critical. J. Fluid Mech. 42, 491. doi:10.1017/S002211207000143X
571 26 Craddock, R.A., Howard, A.D., 2002. The case for rainfall on a warm, wet early Mars. J Geophy Res 107,
572 doi:10.1029/2001JE001505.
573 27 Fisk, M.R., Giovannoni, S.J., 1999. Sources of nutrients and energy for a deep biosphere on Mars. J. Ge-
574 ophys. Res. 104, 11805. doi:10.1029/1999JE900010
575 28 Gupta, S., Collier, J.S., Palmer-Felgate, A., Potter, G., 2007. Catastrophic flooding origin of shelf valley sys-
576 tems in the English Channel. Nature 448, 342–345. doi:10.1038/nature06018
577 29 Gupta, S, Collier, J.S., Garcia-Moreno, D., Oggioni, F, Trentesaux, A., Vanneste, K., De Batist, M.,
578 Camelbeeck, T., Potter, G., Van Vliet-Lanoë, B., Arthur, J.C.R. 2017. Two-stage opening of the Dover
579 Strait and the origin of island Britain. Nat. Commun. 8, 15101 doi: 10.1038/ncomms15101.

30 Hanna, J.C., Phillips, R.J., 2006. Tectonic pressurization of aquifers in the formation of Mangala and Athabasca Valles, Mars. J. Geophys. Res. 111. doi:10.1029/2005JE002546

31 Head, J.W., Wilson, L., Mitchell, K.L., 2003. Generation of recent massive water floods at Cerberus Fossa, Mars by dike emplacement, cryospheric cracking and confined aquifer groundwater release. Geophys Res Lett 30, doi:10.1029/2003GL017135.

32 Horneck, G. 2000. The microbial world and the case for Mars. Planetary and Space Science 48, 1053-1063.

33 Ikeda, H., 1983. Experiments on bedload transport, bed forms, and sedimentary structures using fine gravel in the 4-meter-wide flume: University of Tsukuba, Japan, Environmental Research Centre, Paper 2, 78pp.

34 Jaeger, W.L., Keszthelyi, L.P., McEwen, A.S., Dundas, C.M., Russell, P.S., 2007. Athabasca Valles, Mars: A Lava-Draped Channel System. Science 317, 1709–1711.

35 Jaeger, W.L., Keszthelyi, L.P., Skinner, J.A., Milazzo, M.P., McEwen, A.S., Titus, T.N., Rosiek, M.R., Galuszka, D.M., Howington-Kraus, E., Kirk, R.L., 2010. Emplacement of the youngest flood lava on Mars: A short, turbulent story. Icarus 205, 230–243.

36 Julien, P.Y., Klaassen, G.J., 1995. Sand-dune geometry of large rivers during floods. J. Hydraul. Eng. 121, 657–663. doi:10.1061/(ASCE)0733-9429(1995)121:9(657)

37 Karcz, I., Kersey, D., 1980. Experimental study of free-surface flow instability and bedforms in shallow flows. Sedimentary Geology, 27, 263—300.

38 Keszthelyi, L., Thordarson, T., McEwen, A.S., Haack, H., Guilbard, M.-N., Self, S., Rossi, M.J., 2004. Icelandic analogs to Martian flood lavas. Geochem Geophys Geosys 5, doi:10.1029/2004GC000758.

39 Kirk, R.L., Howington-Kraus, E., Redding, B., Galuszka, D. , Hare, T.M., Archinal, B. A., Soderblom, L. A., Barrett, J. M. 2003. High-resolution topomapping of candidate MER landing sites with Mars Orbiter Camera narrow-angle images, J. Geophys. Res., 108, 8088, doi:10.1029/2003JE002131, E12.

40 Kirk, R.L., E. Howington-Kraus, M.R. Rosiek, J.A. Anderson, B.A. Archinal, K.J. Becker, D.A. Cook, et al. 2008. Ultrahigh Resolution Topographic Mapping of Mars with MRO HiRISE Stereo Images: Meter-Scale Slopes of Candidate Phoenix Landing Sites. J. Geophy. Res. 113, E00A24, doi:10.1029/2007JE003000.

41 Kleinhans, M.G., 2005. Flow discharge and sediment transport models for estimating a minimum timescale of hydrological activity and channel and delta formation on Mars. J Geophy Res 110, doi:10.1029/2005JE002521.

42 Komar, P.D., 1979. Comparisons of the hydraulics of water flows in Martian outflow channels with flows of similar scale on Earth. Icarus 37, 156—181

611 43 Komar, P.D., 1980. Modes of sediment transport in channelized water flows with ramifications to the
612 erosion of the Martian outflow channels. Icarus 42, 317-329.
613 44 Leask, H.J., Wilson, L., Mitchell, K.L., 2006. Formation of Ravi Vallis outflow channel, Mars: Morphological
614 development, water discharge, and duration estimates. J. Geophys. Res. 111.
615 doi:10.1029/2005JE002550
616 45 Leverington, D.W., 2011. A volcanic origin for the outflow channels of Mars: Key evidence and major im-
617 plications. Geomorphology 132, 51–75. doi:10.1016/j.geomorph.2011.05.022
618 46 Malin, M.C., Edgett, K.S., 2001. Mars Global Surveyor Mars Orbiter Camera: Interplanetary cruise through
619 primary mission. J Geophys Res 106, 23,429–23,570.
620 47 Manga, M., 2004. Martian floods at Cerberus Fossae can be produced by groundwater. Geophys Res Lett
621 31, doi:10.1029/2003GL018958.
622 48 McEwen, A.S., Eliason, E.M., Bergstrom, J.W., Bridges, N.T., Hansen, C.J., Delamere, W.A., Grant, J.A., Gu-
623 lick, V.C., Herkenhoff, K.E., Keszthelyi, L.P., Kirk, R.L., Mellon, M.T., Squyres, S.W., Thomas, N., Weitz,
624 C.M., 2007. Mars Reconnaissance Orbiter's High Resolution Imaging Science Experiment (HiRISE). J Geo-
625 phys Res 112, doi:10.1029/2005JE002605.
626 49 McIntyre, N., Warner, N.H., Gupta, S., Kim, J.-R., Muller, J.-P., 2012. Hydraulic modeling of a distributary
627 channel of Athabasca Valles, Mars, using a high-resolution digital terrain model. J. Geophys. Res. 117.
628 doi:10.1029/2011JE003939
629 50 Murray, J., J-P. Muller, Neukum, G., Werner, S.C., van Gasselt, S., Hauber, E., Markiewicz, W.J., Head, J.W.,
630 Foing, B.H., Page, D., Mitchell, K.L., Portyankina, G., the HRSC CoI team, 2005. Evidence from the Mars
631 Express High Resolution Stereo Camera for a frozen sea close to Mars' equator. Nature 434, 352–355.
632 51 Okubo, C.H., 2010. Structural geology of Amazonian-aged layered sedimentary deposits in southwest Can-
633 dor Chasma, Mars, Icarus, 207 (1), 210-225.
634 52 Plescia, J.B., 2003. Cerberus Fossae, Elysium, Mars: a source for lava and water. Icarus 164, 79–95.
635 53 Pollack, J.B., Kasting, J.F., Richardson, S.M., Poliakoff, K., 1987. The case for a wet, warm climate on early
636 Mars. Icarus 71, 203–224.
637 54 Richardson, K., Carling, P.A., 2005. A Typology of Sculpted Forms in Open Bedrock Channels, Geological
638 Society of America Special Paper 392.
639 55 Rubin, D.M., Ikeda, H. 1990. Flume experiments on the alignment of transverse, oblique, and longitudi-
640 nal dunes in directionally varying flows. Sedimentology 37, 673-684.
641 56 Smith, H.D., McKay, C.P. 2005. Drilling in ancient permafrost on Mars for a second genesis of life. Planetary
642 and Space Science 53, 1302-1308

643 57 Tanaka, K.L., Chapman, M.G., 1990. The relation of catastrophic flooding of Mangala Valles, Mars, to fault-
644 ing of Memnonia Fossae and Tharsis Volcanism. J. Geophys. Res. 95, 14315.
645 doi:10.1029/JB095iB09p14315
646 58 van Rijn, L.C., 1984. Sediment transport, Part III: Bed forms and alluvial roughness. J. Hydraul. Eng. 110,
647 1733–1754. doi:10.1061/(ASCE)0733-9429(1984)110:12(1733)
648 59 Vetterlein, J., Roberts, G.P., 2010. Structural evolution of the Northern Cerberus Fossae graben system,
649 Elysium Planitia, Mars. J. Struct. Geol. 32, 394–406. doi:10.1016/j.jsg.2009.11.004
650 60 Wilson, L., Bargery, A.S., Burr, D.M., 2009. Dynamics of fluid flow in Martian outflow channels, in: Burr,
651 D.M., Carling, P.A., Baker, V.R. (Eds.), Megaflooding on Earth and Mars. Cambridge University Press,
652 Cambridge, pp. 290–311.
653

654 **Fig Captions**

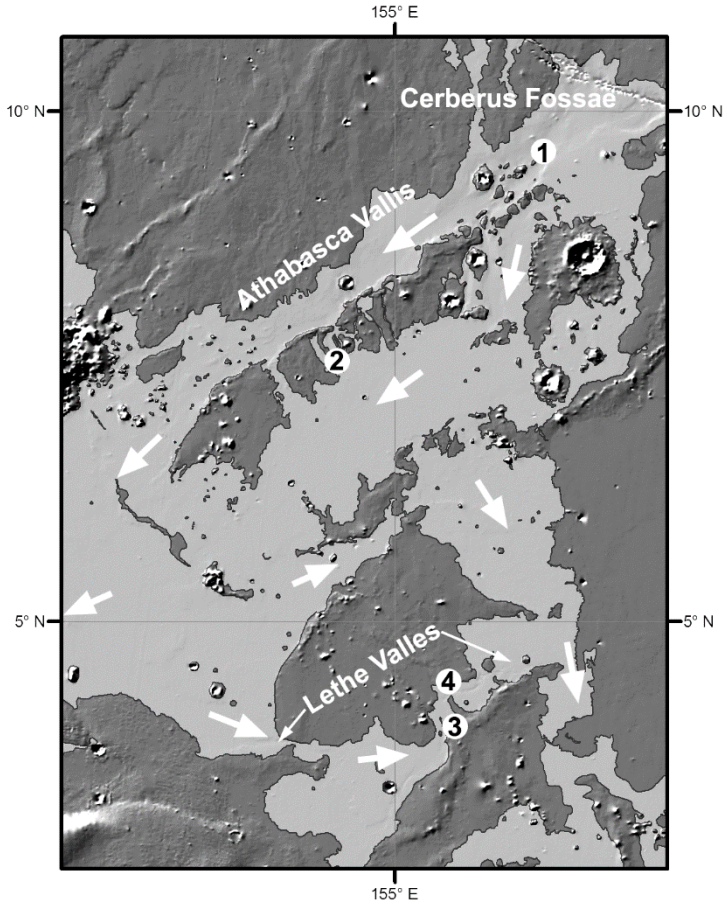

655

656 Fig. 1. Speculated extent of "platy-ridged-terrain" sourced from the Cerberus Fossae and which in-fills topog-
657 raphy (Balme et al., 2010). It is likely that this platy-ridged terrain outlines the extent of past fluvial flooding.
658 White arrows indicate flow directions. The shaded region is equivalent to the maximum ponding extents of
659 the fluid that carved Athabasca Vallis. Numbers show locations of putative fluvial dune study areas.

660

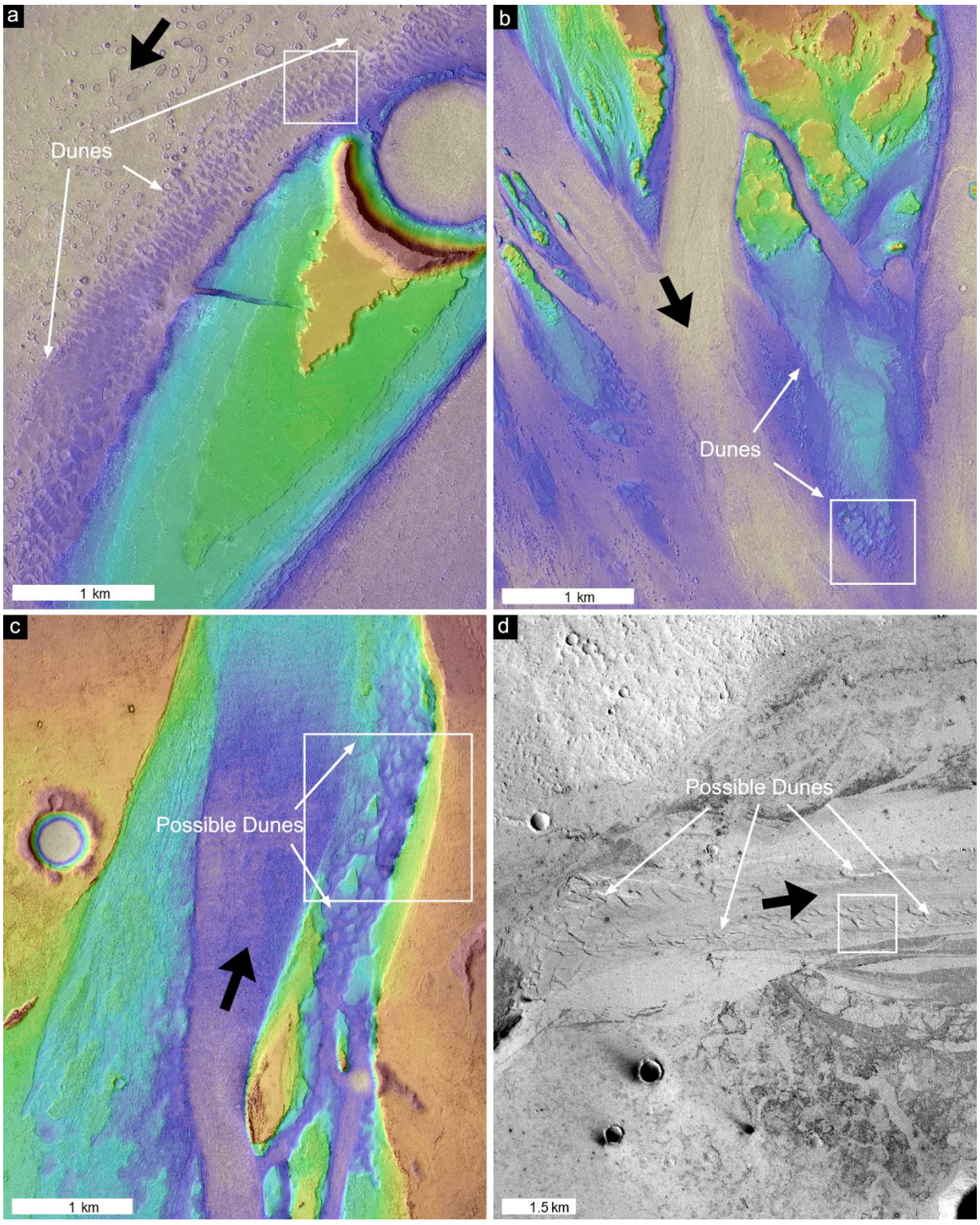

661

662 Fig. 2. Possible dune sites in the Athabasca/Lethe Vallis region. Inferred flow direction of flooding shown by
663 black arrows in all cases. Colour represents topography based on 1 m grid HiRISE DEMs. No stereo HiRISE
664 coverage was available for site 4, so there is not DEM to overlay on the site. Brown shows the highest areas,

and blue/white the lowest. White boxes show locations of detailed views shown in Fig. 4. a. Dunes in Athabasca Vallis, Site 1, identified by Burr et al. (2004). From HiRISE images PSP_002661_1895 and PSP_003294_1895. b. Dunes in an overspill channel that extends perpendicular to Athabasca Vallis (Site 2). From HiRISE images PSP_009768_1880 and PSP_010045_1880. c. Site 3: possible rhomboid dunes in Lethe Vallis – an overspill/return channel from the main Western Elysium Basin. From HiRISE images PSP_006762_1840 and PSP_010335_1840. d. Possible dunes further down Lethe Vallis (site 4). From CTX image D08_030365_1843. North is up in all images and in all following images unless otherwise stated. Image credits NASA/JPL/UofA/MSSS.

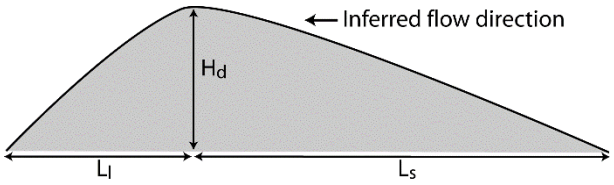

674

675 Fig. 3. Schematic cross-section through a dune and the measurements made from the remote sensing data.
676 H_d is the dune height, L_s the stoss length, L_l the lee length. The total length of the dune is L and is simply L_s+L_l.
677 These parameters are used in Table 2.

678

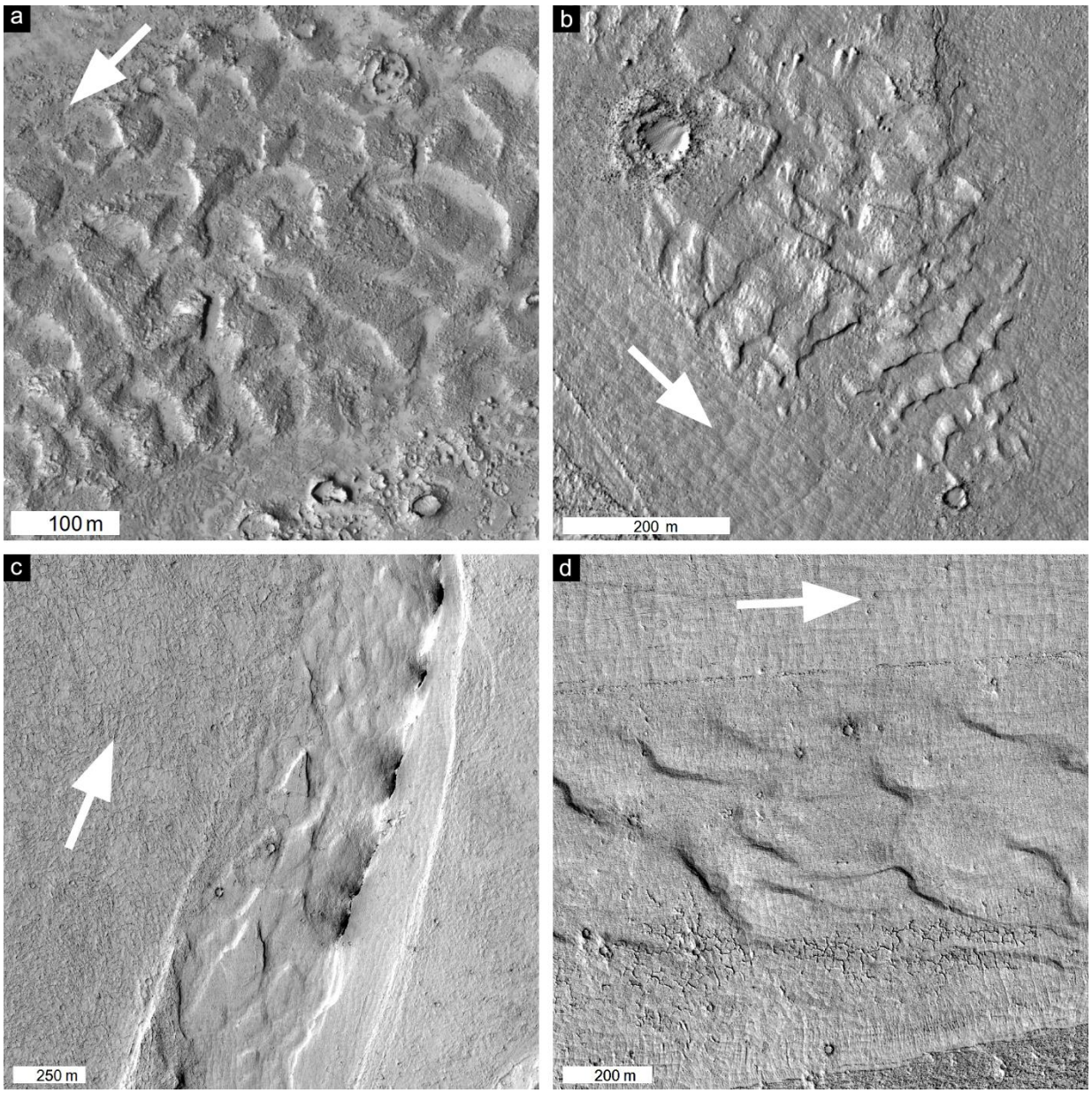

679

680 Fig. 4. Morphology of the putative dunes as seen in HiRISE images. White arrows shows inferred flow direc-
681 tion of dune-forming floods. a. Site 1 dune example. The bedforms are wide (compared to their downstream
682 length) and their crests are gently sinuous in plan-view. The crest to crest distances are usually < 100 m. Note
683 the rough surface texture of both the dunes and many inter-dune areas. Oval/round features are RMLs as
684 described in the text. Part of HiRISE image PSP_002661_1895. b. Site 2 dune example. This area contains
685 features with the most dune-like morphology. Again, the bedforms are wide and have gently sinuous ridge-
686 crests. The crest to crest distances are usually ~ 100 m. The areas in and around the bedforms have a distinc-
687 tive polygonal texture. The polygons occur at different scales, with wavelengths being 2-30 m. The smallest
688 versions of this pattern are also seen on the upstream sides of the dunes themselves. Part of HiRISE image
689 PSP_009768_1880. c. Site 3 dune example. This area contains contiguous rhomboid forms, each with a gently
690 sloping upstream face and a steeper downstream face. Some of the features have a more triangular shape,
691 others are rhomboid but we describe them all as 'rhomboid'). The points of the rhomboid point downstream.
692 The lengths of the rhomboid features range from ~ 100 m to ~ 250 m. The surfaces of these rhomboid forms

693 contain subtly polygonal pattern, similar to site 2, and also lineations and grooves, usually < 1m across and
694 tens or sometimes hundreds of metres long. Part of HiRISE image PSP_006762_1840. d. Site 4 possible dune
695 example. These features are larger than those in sites 1 and 2, being ~ 200m in length, and are oriented
696 obliquely to the downstream direction. They do not have the simple transverse ridge-crest pattern seen in
697 sites 1 and 2, but do have steeper downstream faces compared to upstream. Polygonal patterned surfaces
698 bearing lineations are seen on these features, similar to site 3. Part of HiRISE image ESP_030365_1845. All
699 images credit NASA/JPL/UofA.

700

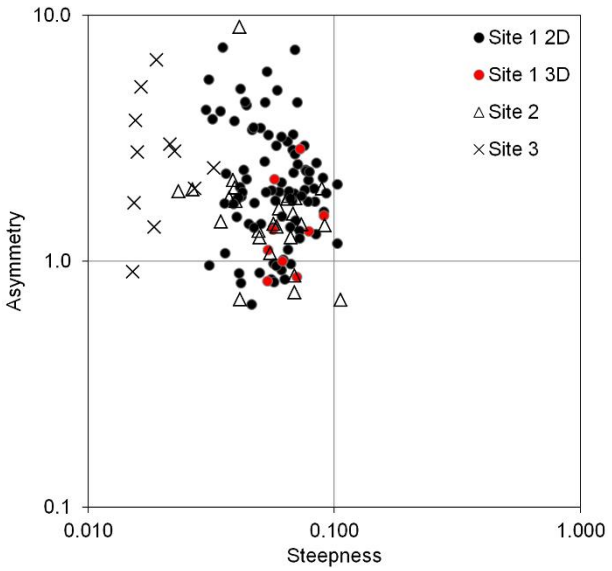

Fig. 5. Shapes of dune forms in Sites 1-3. Asymmetry (stoss length divided by lee length) is plotted against steepness (dune height divided by dune total length). Note that the majority of the features have asymmetry >1 indicating longer stoss than lee slopes, and that there are a significant proportion of significantly asymmetric (>4) features in the dataset. The site 1 and site 2 features occupy similar areas in this parameter space but the Site 3 'rhomboid' dunes are significantly flatter, with a much lower ratio of height to length (steepness).

709 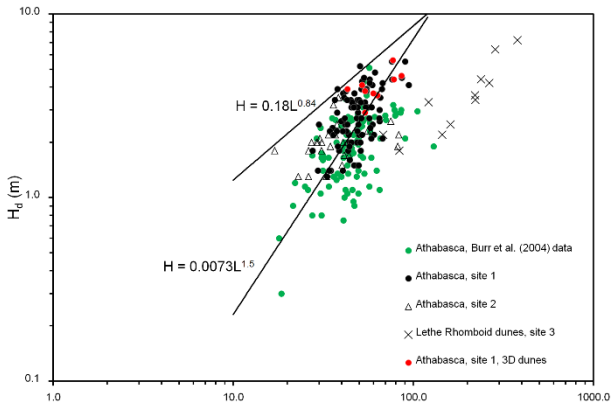

710 Fig. 6. Height vs. length plot of dune forms measured in this study, compared with similar data for site 1 from
711 Burr et al. (2004). Also shown are equations (4) and (5) from Carling (1999) as described in the text (Section
712 6.2).

713

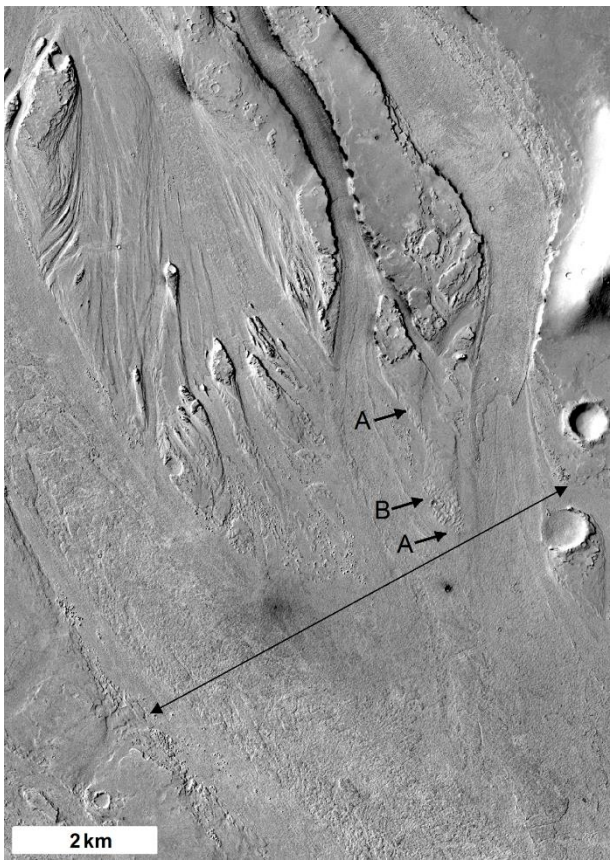

Fig. 7. Site 2 dunes (labelled A, B, C). Fig.4b covers B (the larger, continuous ridge-like 2D dunes) to C (the small, more 3D–style dunes). From A to B there are forms similar in scale to those at B which appear to be bedforms, but do not have a consistent ridge-like shape. The transition from multiple channels at the top of the image to one broad channel at the bottom is clear. The double-arrowed line shows the width of the channel at this point (~ 7km). CTX image B01_010045_1878. Image credit NASA/JPL/MSSS.

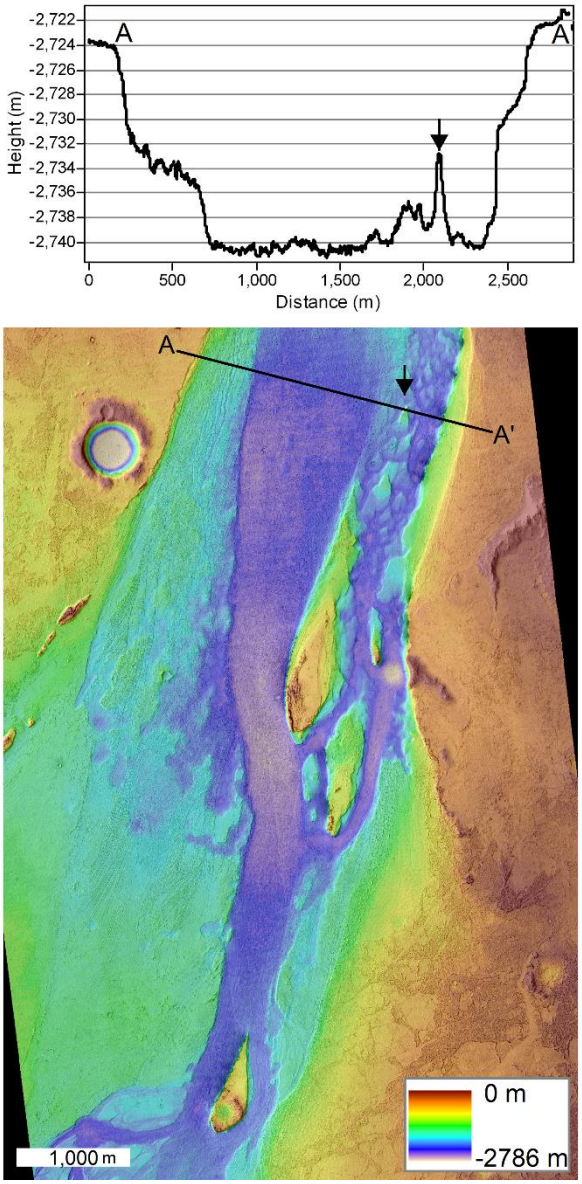

721

722 Fig. 8. HiRISE topography of site 4, part of the Lethe Vallis channel system. Top: topographic profile AA' across
723 the wider channel. The black arrow marks the location of the tallest putative rhomboid dune. Subtle terraces
724 can be seen as inflexions or steps in the profile. Below: HiRISE DEM overlain on a HiRISE orthoimage. The
725 location of the topographic profile AA' is shown, as is the location of the large dune candidate (black arrow).
726 Flow was south to north (bottom to top of the image). Note the streamlined islands and the well-defined
727 inner channel within the broader Lethe Vallis.

728

729

730